Electronic energy loss of slow protons channeled in metals

J. E. Valdés and P. Vargas
Departamento de Física, Universidad de Santiago de Chile, Casilla 307, Santiago, Chile

N. R. Arista
División Colisiones Atómicas, Instituto Balseiro, Centro Atómico Bariloche, 8400 Bariloche, Argentina
(Received 22 April 1997)

The electronic energy loss for low-velocity protons channeled in the ⟨100⟩ direction of single-crystal Au and Al is calculated. The proton trajectories are determined by solving the equation of motion. In the proton dynamics two forces are included, a repulsive term arising from the nuclei and core electrons and a friction force, depending on proton velocity, arising from the valence electrons. The repulsive force on the proton is evaluated using a superposition of conservative potentials. The friction coefficient is evaluated by using the local density of valence electrons, and a quantum-mechanical transport cross-section approach with a self-consistent model based on Friedel's sum rule. The results allow us to describe the nonlinear behavior of energy loss with ion velocity observed experimentally in Au, as well as the linear behavior observed in Al. [S1050-2947(97)05311-0]

PACS number(s): 61.85.+p, 34.50.−s

INTRODUCTION

The problem of ion-solid interactions in the low-energy range is a subject of great interest for studies on radiation damage in solids, ion implantation, surface processes, and other applications. In addition, this is one of the areas where the development of theoretical models still poses several difficult questions [1].

Theoretical calculations of the stopping power of slow ions predict, in the case of metallic targets, a simple proportionality with the ion velocity [2,3]. However, recent experiments with noble metal have shown significant deviations from this prediction, even for the simple case of protons [4–6].

From experimental determination of proton energy loss ΔE by a target of thickness Δx, it is customary to define the friction coefficient as $Q(v)=(1/v)(\Delta E/\Delta x)$, with v being the mean proton velocity [5]. Experiments in monocrystalline Au show a very strong deviation of stopping, namely, $[Q(0.7)-Q(0.2)]/Q(0.7)\approx 50\%$ as shown in Fig. 4 [5]. In polycrystals the deviation is not as strong as in monocrystals, due to multiple scattering and a more uniform and higher, on average, electronic density as compared with a single channel in a monocrystal. In the case of a polycrystalline sample, a deviation of $[Q(0.6)-Q(0.22)]/Q(0.6)\approx 28\%$ is found, which is significant [6]. From the experimental point of view this effect cannot be explained by nuclear stopping or by secondary effects, such as path length enlargement due to multiple scattering, effective foil-thickness variation due to foil roughness, or the accuracy in the thickness determination [11]. The origin of this deviation was explained as arising from the so-called threshold effect in the excitation of d electrons in those metals [11].

On the other hand, in a recent study [7] we have developed a model to simulate the slowing down of channeled protons in a crystalline solid. This model includes a band structure calculation to represent the electronic density within the channel, a simulation of proton trajectories, and the use of a self-consistent model to calculate the electronic energy loss of the channeled protons after the simulation has been performed.

In the present paper we generalize that model by including explicitly a friction term in the dynamic of the proton particles. The electronic structure of the host material is represented through the calculated density of states and electron charge density. The contribution of the different electron bands to the energy loss is evaluated. In order to represent the channeling process we use a molecular-dynamics approach in which the proton trajectories are determined from the classical equations of motion, under the influence of the potential produced by the nuclei and core electrons, and subject also to a dissipative friction force resulting from the interaction with the valence (s, p, and d) electrons.

The friction coefficient is modeled locally by an effective electron density that takes into account only a fraction of valence electrons. This fraction corresponds to the electrons that can be excited by the proton at its instantaneous position. The value of the friction coefficient is evaluated using both a detailed spatial description of the valence electron density of the host and a model for the energy transfer to electrons in a collision.

The energy-loss distributions for protons in channeling, through monocrystalline Au and Al ⟨100⟩, is calculated and the most probable energy loss is compared with experimental data for proton velocities ranging from 0.1 to 1.0 a.u. The experiments show no velocity dependence for the friction coefficient in Al [6] and a strong variation with velocity in the case of Au [4–6]. The model presented here describes very well the energy-loss behavior with velocity in both cases.

I. MODEL

The stopping of a positive ion at low velocities by an electronic gas of uniform density n is usually given by the following relation [8–10]:

$$\frac{dE}{dx} = -Q_e v, \tag{1}$$

where Q_e is the friction coefficient,

$$Q_e(n) = n v_F \sigma_{\rm tr}(n), \tag{2}$$

and $\sigma_{\rm tr}(n)$ is the transport cross section. This model is valid for proton velocities v, which are less than the Fermi velocity of the electrons $v_F = (3\pi^2 n)^{1/3}$. In the free-electron gas the energy and pseudomomentum are related by $\varepsilon(\mathbf{k}) = \hbar^2 \mathbf{k}^2/2m$. This parabolic relationship gives rise to a square root shape for the density of states. In a real metal only the s states are parabolic near the Γ point in the Brillouin zone, and in this sense they can be treated as free for the ion stopping. Other electronic states have no parabolic shape and sometimes they can be very localized below the Fermi level, that is, the case of d electrons in the majority of the transition metals.

Based on these considerations we propose a model for the electronic stopping in solids that takes into account both the local density and the local energy distribution of the electrons in the target host.

The present theoretical model assumes a local approximation for the stopping power as predicted by the free-electron-gas model, for each incident velocity, but with a varying electronic density depending on the region explored by the proton along the channel in its trajectory. At low velocities, the proton channels only if its impact parameter is near the axis; in this region the valence electronic density is low and the stopping power is reduced. As the proton energy increases, it can explore regions further away from the axis without being dechanneled; then, if on average the sampled electronic density is higher, the stopping increases as well.

On the other hand, the electrons in the solid are bounded, so the creation of an electron-hole pair is achieved only if the proton loses a minimum of energy in a binary collision. This energy threshold is the difference between the Fermi energy and the energy of the electronic state of the involved electron. Then, only a fraction of the electrons at the instantaneous proton position can be excited and contribute to the friction coefficient.

Consequently the friction coefficient can be written as

$$Q_e(n_{\rm eff}) = n_{\rm eff} v_e(n_{\rm eff}) \sigma_{\rm tr}(n_{\rm eff}), \tag{3}$$

where the effective electron density $n_{\rm eff}$ is now a local property depending on both the instantaneous proton position and the excitation spectra of the electrons.

On each point, we model the valence electronic density $n_{\rm loc}$, as given by a contribution of s, p, and d electrons, i.e.,

$$n_{\rm loc} = n_s + n_p + n_d, \tag{4}$$

where

$$n_l = \gamma \int_{\varepsilon_0}^{\varepsilon_F} g_l(\varepsilon) d\varepsilon. \tag{5}$$

Here, g_s, g_p, and g_d stand for the l-projected density of states (DOS) of the host material. γ is a volume factor that for fcc structure is $\gamma = 4/a^3$, where a is the lattice parameter.

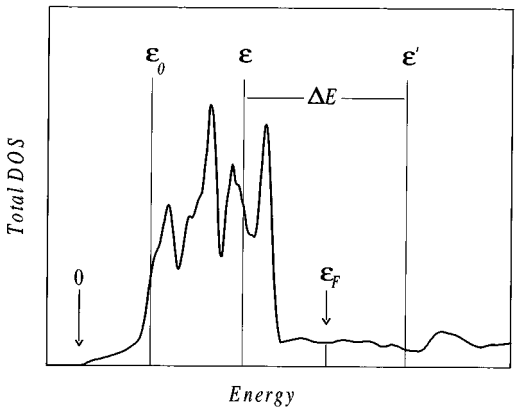

FIG. 1. The figure shows schematically the total DOS for solid Au as a function of electron energy. The zero of energy is defined at the bottom of the bands. ε_0 is calculated locally to adjust the valence electron density $n_{\rm loc}$ and ε_F is the Fermi level. ΔE is an average energy transfer to one electron, with initial energy $\varepsilon \leqslant \varepsilon_F$, to an excited energy level $\varepsilon' > \varepsilon_F$, with $\varepsilon' = \varepsilon + \Delta E$.

If the lower limit of integration, ε_0 in Eq. (5), is taken as 0, then $n_{\rm loc} = n$ is the total number of valence electrons (per unit volume) for a given material. Our model fixes the ε_0 value in such a way that the local electronic density $n_{\rm loc}$ can be written as

$$n_{\rm loc} = \gamma \int_{\varepsilon_0}^{\varepsilon_F} g_{\rm tot}(\varepsilon) d\varepsilon, \tag{6}$$

where $g_{\rm tot}(\varepsilon)$ is the total DOS, $g_{\rm tot} = g_s + g_p + g_d$.

In some locations within the channel, primarily near the nuclei, the local charge density can be higher than the average number of valence electrons, (3γ in case of Al and 11γ for Au). In that case, ε_0 is taken equal to zero, i.e., we integrate in the complete bandwidths.

To estimate the threshold energy for non-s electrons we use an average of the energy transfer to a single electron, ΔE, in a binary collision [11]

$$\Delta E = v v_r(n_{\rm loc}) \beta(n_{\rm loc});$$

here β is defined as the average value of $1 - \cos(\theta)$ over the normalized cross-section function,

$$\beta(n_{\rm loc}) = \frac{\int |f(\theta)|^2 [1 - \cos(\theta)] d\Omega}{\int |f(\theta)|^2 d\Omega}, \tag{7}$$

where $f(\theta)$ is the scattering amplitude that depends on electronic density through the phase shifts, and $v_r(n_{\rm loc})$ is the average of the relative velocity of the electrons over the total density of states, given by

$$v_r(n_{\rm loc}) = \frac{1}{n_{\rm loc}} \int_{\varepsilon_0}^{\varepsilon_F} \gamma g_{\rm tot}(\varepsilon) v_r(\varepsilon) d\varepsilon. \tag{8}$$

Here $v_r(\varepsilon)$ is given by the usual expression [12]

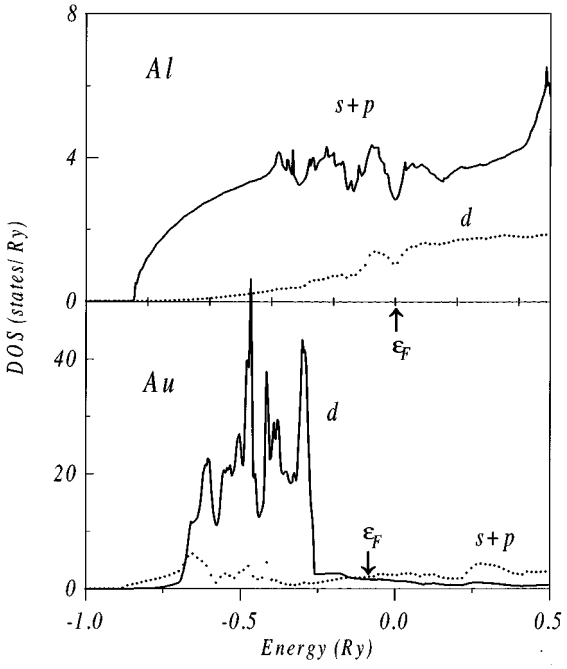

FIG. 2. Density of electronic states in fcc Al ($a=4.05$ Å) and fcc Au ($a=4.08$ Å) as a function of energy calculated by the linear muffin-tin orbital method [14,15]. The upper panel shows the partial DOS for $s+p$ (solid line) and d (dotted line) electrons for Al. The lower panel shows partial $s+p$ (dotted line), and d (solid line) DOS in case of Au. The position of the Fermi energy ε_F is indicated by an arrow in both cases. We clearly see that the d electrons play almost no role in the case of Al, whereas in Au their role is crucial, giving an important contribution to electronic energy loss for protons in channeling experiments.

$$v_r(\varepsilon)=\frac{v_e^2}{6v}\left[\left(\frac{v}{v_e}+1\right)^3-\left|\frac{v}{v_e}-1\right|^3\right]. \tag{9}$$

v_e is the free electron velocity, (i.e., $v_e^2=2\varepsilon$ in a.u.).

Once we estimate ΔE in every step of the simulation, we compare this energy with the bandwidth $(\varepsilon_F-\varepsilon_0)$ of the valence electrons. On average the proton will lose an energy ΔE, and this energy will raise the energy of an electron to a state over the Fermi level. To proceed with the calculations we include the energy loss on the motion of the channeled protons by assuming a random occurrence of excitation processes, where electrons with energies $\varepsilon<\varepsilon_F$ absorb, on the average, an energy ΔE, and consider only those events where the final energy $\varepsilon'=\varepsilon+\Delta E$ is above the Fermi level $(\varepsilon'>\varepsilon_F)$. In this way we take into account the *threshold effect* in the energy loss [11]. Figure 1 indicates the different energy variables cited above. The detail of the calculated s, p, and d electron density of states for the cases of Al and Au are shown in Fig. 2.

Depending on the ε value we can have three situations: first, if $\varepsilon>\varepsilon_0$, $n_{\rm eff}$ is given by

$$n_{\rm eff}=n_s+n_p+\gamma\int_{\varepsilon}^{\varepsilon_F} g_d(\varepsilon'')d\varepsilon''. \tag{10}$$

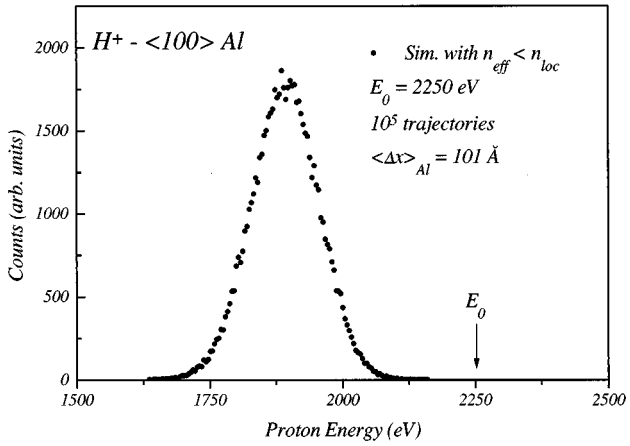

FIG. 3. Typical energy-loss distribution for protons emerging from channel $\langle 100\rangle$ in Al. The simulation was done using over 10^5 trajectories with random incident impact parameters with respect to the channel axis. The protons incident velocity is 0.3 a.u. ($\sim$2.25 keV) and the average channel length was $\langle\Delta x\rangle=25a$ ($a=4.05$ Å).

In this case $n_{\rm eff}<n_{\rm loc}$, and this expression gives us the effective density of electrons that participate in the proton energy loss process and will be considered as nearly free electrons in Eq. (3).

The second possibility is $\varepsilon\leqslant\varepsilon_0$. In this case we take all the local density electrons participating in the stopping power, that is,

$$n_{\rm eff}=n_{\rm loc}=n_s+n_p+n_d. \tag{11}$$

The third situation is $\varepsilon\geqslant\varepsilon_F$. In that case the energy level ε is unoccupied, and therefore

$$n_{\rm eff}=0. \tag{12}$$

Finally, in any case, the local friction constant is given by Eq. (3).

Simulation of proton trajectories

The simulation of proton trajectories was done by solving the motion equation for a proton moving under the effect of two forces, the first arising from a repulsive potential that models the metallic nuclei and electron cores, and second, the dissipative force given by Eq. (1), using the friction coefficient of Eq. (2) [7]. Numerical solutions of the motion equations are done using a Runge-Kutta method of order 4 with adaptive time steps [13]. The practical calculation of the electron density is carried out using the tight-binding linear muffin-tin orbitals (TB-LMTO) method [14,15]. Here, the valence electronic density is evaluated for the metal in a regular mesh of $64\times64\times64$ points in the unit cell.

The dynamical simulations of the trajectories are repeated for proton velocities in the range of $0.1-1.0$ a.u, i.e., they were experimentally the energy loss for protons in Au $\langle 100\rangle$ and in polycrystalline Al were measured. A number of 10^5 histories was simulated for each proton velocity. The simulated channel length was $25a$ ($\sim$100 Å). A typical spectrum of emerging particles is shown in Fig. 3.

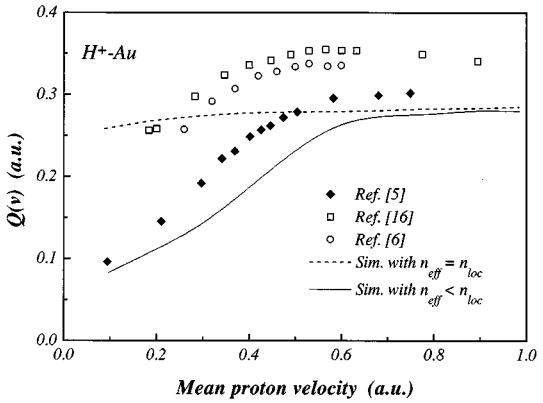

FIG. 4. Friction coefficient Q for protons in Au as a function of the mean proton velocity in atomic units. The open squares [16] and circles [6] are the data obtained from experimental proton energy-loss measurements in polycrystalline Au thin films. The solid diamonds show the experimental values for protons channeled in ⟨100⟩ Au [5]. The dashed line shows the result of the simulation for the electronic friction coefficient in Eq. (3) considering that $n_{\mathrm{eff}}=n_{\mathrm{loc}}$, without energy threshold effect, for protons channeled in ⟨100⟩ Au. The solid line represents the Q value obtained from a simulation including the threshold effect.

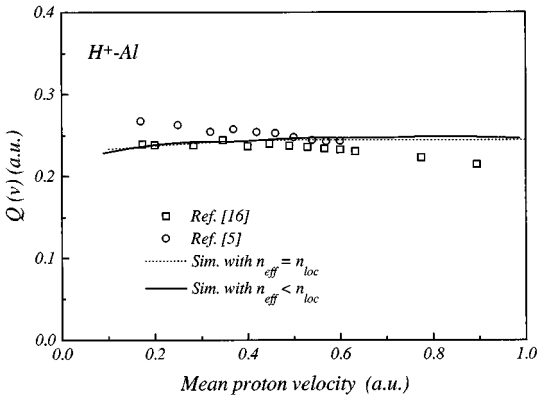

FIG. 5. Friction coefficient Q for protons in Al as a function of the mean proton velocity in atomic units. The open squares [16] and circles [6] represent those values obtained from experimental proton energy-loss measurements in polycrystalline Al thin films. The dashed line shows the result of the simulation for the electronic friction coefficient in Eq. (3) considering that $n_{\mathrm{eff}}=n_{\mathrm{loc}}$, without energy threshold effect for protons channeled in ⟨100⟩ Al. The solid line represents the Q values given by the present simulation, including an energy threshold for d electrons.

II. RESULTS

Figure 4 shows the friction coefficient Q for protons in Au as a function of the mean proton velocity in atomic units. The open squares [16] and circles [6] represent the Q values obtained from experimental proton energy loss measurements in polycrystalline Au thin films. The solid diamonds show the experimental friction coefficient for protons channeled in Au ⟨100⟩ [5]. The dashed line shows the result of the simulation for the electronic friction coefficient Q in Eq. (3) considering that $n_{\mathrm{eff}}=n_{\mathrm{loc}}$, without energy threshold effect, for protons channeled in Au ⟨100⟩. The small deviation from a straight line at the lowest velocities is produced by the hyperchanneling effect (proton trajectories very close to the channel axis, where the electronic density is lowest). The solid line represents the Q value obtained from further simulations, but including the threshold effect on the excitation of d electrons according to Eqs. (10), (11), and (12). The contribution of f electrons is negligible, because of its small occupation fraction (see Discussion section).

Figure 5 shows the results for the friction coefficients obtained for protons in Al. The open squares [16] and circles [6] represent the Q values obtained from experimental proton energy-loss measurements in polycrystalline Al thin films. One can see that the experimental Q value is approximately constant as a function of the mean projectile velocity. This indicates a free-electron-like behavior for the electronic stopping power for protons in Al . The dashed line shows the result of the simulation for the electronic friction coefficient Q in Eq. (3) considering that $n_{\mathrm{eff}}=n_{\mathrm{loc}}$, without energy threshold effect, for protons channeled in Al ⟨100⟩. The solid line represents the Q values given by the present theoretical model calculated for proton in Al ⟨100⟩, including an energy threshold for d electrons. Both theoretical curves are approximately equal because of the small occupation fraction of d electrons in solid Al.

III. DISCUSSION

By comparing the Q values, which have been calculated from the simulation of proton trajectories, with the experimental Q values shown in Figs. 4 and 5 we observe excellent agreement between the theoretical model and the experiments. In the case of polycrystalline Au, the experiment shows higher stopping than that of monocrystalline Au in the ⟨100⟩ direction. This can be explained on the basis that the average electron density is higher in the polycrystal, and that the nuclear stopping is also higher. However, the behavior of Q with proton velocity is similar in both cases, indicating that this is an effect of the electronic structure of Au rather than of the crystal structure.

The energy loss due to momentum transfer to nuclei is not contained in our model, since the force on the proton arising from nuclei and core electrons is modeled by a conservative potential, and nuclei remain fixed. However, the nuclear stopping is smaller than the electronic stopping in channeling conditions and should be smaller in Au than in Al due to their atomic mass differences. We observe that in Au, the Q values obtained by the simulation are always low approximately by a constant shift of 10% with respect to the experimental results. This deviation may be explained, among other causes (thickness determinations, crystalline defects, structural disorder, and angular acceptance in the detection procedure) by nuclear energy loss. Presently we are investigating the inclusion of nuclear stopping in our simulation model.

The occupation of the electronic states for electrons in solid Au is $5d^{9.31}5f^{0.14}6s^{0.8}\,6p^{0.75}$ as obtained from the TB-LMTO calculation for fcc Au with a lattice parameter of 4.08 Å. In solid fcc Al with a lattice parameter of 4.05 Å the electronic configuration is $3s^{1.2}3p^{1.45}\,3d^{0.35}$. We clearly see that the role of the localized d electrons in Au is much more important than in Al due to its high electron population. Moreover, in Al the spatial distribution of valence electrons

in the ⟨100⟩ channel is more homogeneous than that of Au ⟨100⟩. This explains why the Q values obtained for Al are very insensitive to proton velocity and also why the energy threshold for d electrons plays almost no role.

On the other hand, to our knowledge, there are no measurements of proton energy loss in Al monocrystals in the ⟨100⟩ direction for velocities in the range 0.1–1.0 a.u. However, the experimental results for polycrystalline Al are very similar to those of the simulation in channeling conditions. This is a consequence of the higher spatial uniformity of the electron density in solid Al than in solid Au. Then, averaging quantities depending on the valence electron density over different directions in Al, so as to emulate polycrystal, will give similar results to those calculated in one particular direction. This is not the case for Au, as discussed above.

IV. CONCLUSION

According to the obtained results and based on the theoretical framework of the model we conclude the following.

The dynamical simulation of proton trajectories including both a periodic repulsive potential together with a dissipative term arising from the excitation of valence electrons allows us to explain the energy loss of channeled protons in metals.

The present model contains no free parameters, and incorporates the electronic band structure of each element through a realistic calculation of the spatial distribution of valence electrons and electronic density of states.

The friction constant of the dissipative force includes two main effects: the spatial inhomogeneities of the electron density and a minimum excitation energy for localized electrons in the host. These two effects are crucial to our understanding of the experimental energy loss for protons channeled in thin metallic films at low velocities.

Comparisons of the friction coefficients obtained with the present model with experimental available data in fcc Au and fcc Al show very good agreement, which indicates that the present model may be extended to the case of polycrystalline solids and semiconductors.

ACKNOWLEDGMENTS

Financial support from DICYT of the Universidad de Santiago de Chile and the Argentine-ICTP Scientific Cooperation Program is gratefully acknowledged. Hospitality from the CAB and useful discussions with J. C. Eckardt and G. H. Lantschner are also acknowledged.

[1] A. Gras-Martí, H. M. Urbassek, N. R. Arista, and F. Flores, *Interaction of Charged Particles with Solid and Surfaces*, Vol. 271 of *NATO Advanced Study Institute, Series B: Physics* (Plenum, New York, 1991).
[2] W. Brandt, Nucl. Instrum. Methods **191**, 453 (1981).
[3] M. A. Kumakhov and F. F. Komarov, *Energy Loss and Ion Ranges in Solid* (Gordon and Breach, New York, 1979).
[4] G. Högberg, H. Norden, and R. Skoog, Phys. Status Solidi **42**, 441 (1970).
[5] R. Blume, W. Eckstein, H. Verbeek, and K. Reichlet, Nucl. Instrum. Methods **194**, 67 (1982).
[6] J. E. Valdés, G. Martínez, G. H. Lantschner, J. C. Eckardt, and N. R. Arista, Nucl. Instrum. Methods Phys. Res. B **73**, 313 (1993).
[7] P. Vargas, J. E. Valdés, and N. R. Arista, Phys. Rev. A **53**, 1638 (1996).
[8] T. L. Ferrell and R. H. Ritchie, Phys. Rev. B **16**, 115 (1977).
[9] E. Bonderup (unpublished).
[10] P. M. Echenique, I. Nagy, and A. Arnau, Int. J. Quantum Chem. **23**, 521 (1989).
[11] J. E. Valdés, J. C. Eckardt, G. H. Lantschner, and N. R. Arista, Phys. Rev. A **49**, 1083 (1994).
[12] S. Kreussler, C. Varelas, and W. Brandt, Phys. Rev. B **23**, 82 (1981).
[13] W. H. Press, S. A. Teukolsky, W. T. Vetterling, and B. P. Flannery, *Numerical Recipes in C*, 2nd ed. (Cambridge, Oxford, 1992).
[14] O. K. Andersen and O. Jepsen, Phys. Rev. Lett. **53**, 2571 (1984).
[15] O. K. Andersen, Z. Pawlowska, and O. Jepsen, Phys. Rev. B **34**, 5253 (1986).
[16] G. Martínez-Tamayo, J. C. Eckardt, G. H. Lantschner, and N. R. Arista, Phys. Rev. A **54**, 3131 (1996).